ARMY RESEARCH LABORATORY

Viscoelastic Characterization of Aliphatic Polyurethane Interlayers

by Neil MacAloney, Andres Bujanda, Robert Jensen, and Nakhiah Goulbourne

ARL-TR-4296   **October 2007**

NOTICES

Disclaimers

The findings in this report are not to be construed as an official Department of the Army position unless so designated by other authorized documents.

Citation of manufacturer's or trade names does not constitute an official endorsement or approval of the use thereof.

Destroy this report when it is no longer needed. Do not return it to the originator.

Army Research Laboratory

Aberdeen Proving Ground, MD 21005-5069

Viscoelastic Characterization of Aliphatic Polyurethane Interlayers

Neil MacAloney and Nakhiah Goulbourne
Virginia Polytechnic Institute and State University

Andres Bujanda and Robert Jensen
Weapons and Materials Research Directorate, ARL

REPORT DOCUMENTATION PAGE			Form Approved OMB No. 0704-0188
Public reporting burden for this collection of information is estimated to average 1 hour per response, including the time for reviewing instructions, searching existing data sources, gathering and maintaining the data needed, and completing and reviewing the collection information. Send comments regarding this burden estimate or any other aspect of this collection of information, including suggestions for reducing the burden, to Department of Defense, Washington Headquarters Services, Directorate for Information Operations and Reports (0704-0188), 1215 Jefferson Davis Highway, Suite 1204, Arlington, VA 22202-4302. Respondents should be aware that notwithstanding any other provision of law, no person shall be subject to any penalty for failing to comply with a collection of information if it does not display a currently valid OMB control number. **PLEASE DO NOT RETURN YOUR FORM TO THE ABOVE ADDRESS.**			
1. REPORT DATE (DD-MM-YYYY) October 2007	**2. REPORT TYPE** Final		**3. DATES COVERED (From - To)** December 2006–June 2007
4. TITLE AND SUBTITLE Viscoelastic Characterization of Aliphatic Polyurethane Interlayers			**5a. CONTRACT NUMBER** W911NF-06-2-0014
			5b. GRANT NUMBER
			5c. PROGRAM ELEMENT NUMBER
6. AUTHOR(S) Neil MacAloney,* Andres Bujanda, Robert Jensen, and Nakhiah Goulbourne*			**5d. PROJECT NUMBER** AH42
			5e. TASK NUMBER
			5f. WORK UNIT NUMBER
7. PERFORMING ORGANIZATION NAME(S) AND ADDRESS(ES) U.S. Army Research Laboratory ATTN: AMSRD-ARL-WM-MA Aberdeen Proving Ground, MD 21005-5069			**8. PERFORMING ORGANIZATION REPORT NUMBER** ARL-TR-4296
9. SPONSORING/MONITORING AGENCY NAME(S) AND ADDRESS(ES)			**10. SPONSOR/MONITOR'S ACRONYM(S)**
			11. SPONSOR/MONITOR'S REPORT NUMBER(S)
12. DISTRIBUTION/AVAILABILITY STATEMENT Approved for public release; distribution is unlimited.			
13. SUPPLEMENTARY NOTES *Virginia Polytechnic Institute and State University, Blacksburg, VA 24061			
14. ABSTRACT The viscoelastic properties of several commercially available aliphatic thermoplastic polyurethanes were characterized. Differential scanning calorimetry showed that for Deerfield 4700, Inter Materials IM 800, IM 800A, IM 1600, and IM 2500, there is a permanent physical change that occurs during heating. Dynamic mechanical analysis and shear rheometry were used to generate elastic and shear modulus master curves in the frequency domain for Inter Materials IM 800 A. The Williams-Landel-Ferry constants and Prony coefficients were extracted from these master curves. Quasi-static mechanical properties were determined from tensile tests on dog bone samples and compression tests on cylindrical samples. Visual image correlation was used to determine the Poisson's ratio from the mechanical tests by simultaneously capturing longitudinal and lateral strain.			
15. SUBJECT TERMS thermoplastic polyurethane, viscoelasticy, Prony coefficients, interlayer, transparent, aliphatic polyurethane			
16. SECURITY CLASSIFICATION OF:	**17. LIMITATION OF ABSTRACT**	**18. NUMBER OF PAGES**	**19a. NAME OF RESPONSIBLE PERSON** Andres Bujanda

a. REPORT UNCLASSIFIED	**b. ABSTRACT** UNCLASSIFIED	**c. THIS PAGE** UNCLASSIFIED	UL	36	**19b. TELEPHONE NUMBER** (Include area code) 410-306-1910

Contents

List of Figures

List of Tables

Acknowledgments

1. Introduction

Transparent laminate structures have a multitude of uses in modern structural and vehicular applications. These multilayered systems comprise multiple materials bonded by polymer interlayers. These dissimilar materials are used in laminate structures to increase the performance and decrease the weight of the structure. The interlayer serves not only to join layers, but to mitigate stresses due to thermal expansion mismatches and to enhance the impact performance of the structure. The use of interlayers is instrumental in optimizing a laminated composite structure for maximum performance.

Multilayered structures are used in many applications where protection is a factor, so it is important to accurately predict the deformation mechanics of these structures. When loaded at high strain rates, the rate dependent properties in different layers of the structure create a very complex response. Due to these time varying properties of each layer, difficulties arise in developing experimentally valid numerical models (*1*). These difficulties are further augmented by the composite response which is not a linear superposition of the individual laminate response.

In addition to large deformations in the material, compressive, shear, and surface waves propagate from the impact site (*2*). The interaction of these waves creates internal tensile stresses which cause internal damage (*3*). When multiple layers are used, impedance mismatches between layers result in both reflection and transmission of a wave at interfaces. Furthermore, the elastic interlayers significantly alter wave propagation in multilayer structures (*4*).

Many studies have been conducted to characterize the properties of the individual monolithic layers used in multilayered structures, such as polycarbonate or polymethylmethacrylate, however, there has not been such a focus in characterizing the interlayers of these structures. Aliphatic polyurethanes are one type of material used as interlayers in transparent laminates. In this analysis, five different interlayers with varying properties were studied. The commercial polyurethanes studied were Deerfield A4700, and Inter Materials IM 800, IM 800A, IM 1600, and IM 2500.

Experimental methods utilized in this study included differential scanning calorimetry (DSC), dynamic mechanical analysis (DMA), shear rheometry, tensile testing, and compression testing. From the test methods described in this paper, the elastic modulus, shear modulus, and linear viscoelastic properties of the polyurethane interlayer were quantified.

2.   Experimental

2.1   Materials

The focus of this work is on transparent multilayered structures. These structures are assembled with hard layers bonded with compliant polymer interlayers. Since the interlayers have the dual role of both bonding the layers and straining to compensate for thermal mismatches, they are generally constructed of an elastic polymer. A common polymer used in this application is a thermoplastic polyurethane (TPU). Polyurethanes are categorized by the type of isocyanate used in their synthesis and are generally categorized as either aliphatic or aromatic depending on the molecular structure. Aliphatic polyurethanes are generally transparent, due to the absence of benzene rings and are typically used in the manufacture of TPU's. Optical grade aliphatic TPU was obtained from Inter Materials, LLC (Richmond, VA), and Deerfield Urethane, Inc. (Deerfield, MA) as extruded rolled sheet. The product listings and sheet thicknesses are summarized in table 1. These materials are typically extruded into a sheet from resin form using heat. From the sheet form, the laminates are constructed by placing the TPU between the layers, vacuum bagging the assembly, and placing it in an autoclave.

Table 1. Thermoplastic polyurethanes analyzed.

Manufacturer	Product Listing	Thickness (mm)
Deerfield Urethane	A4700	1.27
Inter Materials	800	1.33
Inter Materials	800A	1.27
Inter Materials	1600	1.27
Inter Materials	2500	0.635

2.2   Differential Scanning Calorimeter

The thermal properties of the TPU's were tested using a TA Instruments Q1000 differential scanning calorimeter (DSC). Samples were equilibrated at a temperature of –60 °C for 5 min. The temperature was increased at a rate of 10 °C per min to a temperature of 120 °C. After holding the sample at this temperature for 5 min, the temperature was decreased again to –60 °C and held for 5 min. The temperature was increased again at the same rate to 120 °C. A diagram of the temperature sweep is shown in figure 1. Figure 2 shows the heat flow from the heats for each TPU. It should be noted that typical thermal profiles for laminated assemblies involve much slower heating rates and longer isothermal soak durations.
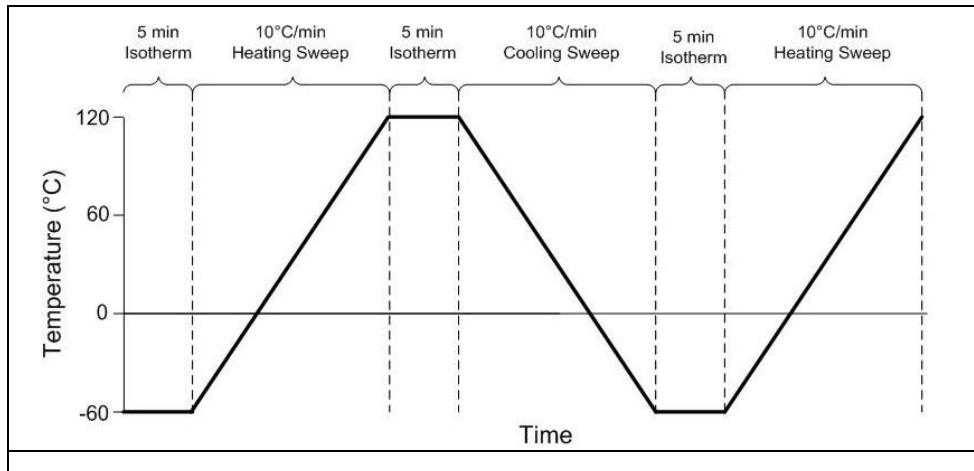
Figure 1. Experimental temperature ramp profile used for the DSC characterization.
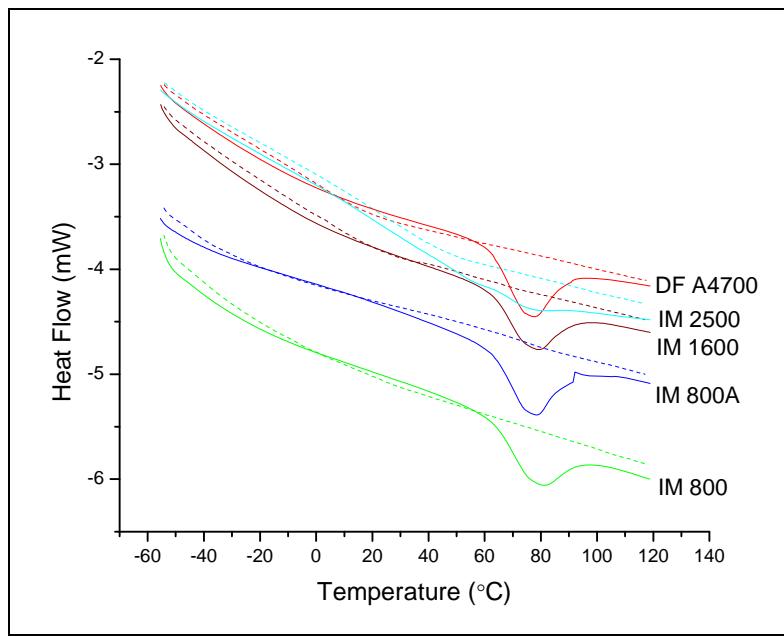
Figure 2. First (solid) and second (dashed) heat DSC results for the TPU's.

From the solid lines on the above DSC plots, it is clear that there is an endothermic event that takes place in all TPU's in the first heat between 60 and 100 °C. The second heat, as illustrated by the dashed lines in figure 2, shows no endothermic event. This indicates that there is a permanent change that takes place during the first heat.

Thermoplastic polyurethanes are made from of two different blocks in a repeating linear polymer. The two sections are generally referred to as hard and soft segments. At the polymer's usage temperature, the soft segment is in a rubbery phase while the hard segment is in a crystalline state (5). At first glance, it is plausible that the endotherm seen in the thermogram of

transparent polyurethanes represents the melting temperature of the hard segments in the polyurethane. However, no subsequent recrystallization exotherms or melting endotherms were observed in the DSC during repeated cooling and heating cycles.

Initially, the TPU sheets are semi-transparent (figure 3). When the polyurethane is heated past 60 °C, it becomes optically transparent (figure 4) with a marked change in surface texture. The increase in transparency was determined to be caused by surface melting in the polyurethane; the as drawn polyurethane can be made transparent by immersing it in water. TPU sheets are provided with a matte finish that allows air to escape when the assembly is heated in an autoclave. In addition to the surface melting upon heating, the polyurethane contracts in the draw direction. To quantify the amount of contraction during heating, the dimensions of a sample were measured before and after thermal annealing. A small square (30.48×30.48 mm) of IM 800A was heated in a Blue M Electric Model DC-206C oven for 2 hr at 120 °C. After heating, the specimen contracted in the draw direction by ~33%, increased perpendicular to the draw direction by 5% and increased in thickness 22% while maintaining a constant volume. This constant volume process, which is observed as the endotherm in the DSC, indicates the contraction is an artifact of annealing and does not constitute a significant event.

Figure 3. As-drawn aliphatic polyurethane.

Polymers that are processed at elevated temperature and cooled rapidly can take on a non-equilibrium state (6). This occurs when the molecular relaxation rate of the polymer cannot keep pace with the surrounding environment to maintain thermodynamic equilibrium. Similarly, since the TPU studied is processed at an elevated temperature and cooled rapidly after extrusion, it can be in a non-equilibrium state and may be susceptible to physical ageing, which is accelerated with increased temperature. By thermally annealing the polymer, internal relaxations occur at a faster rate, changing its morphology and consequently, its mechanical properties. When the TPU is incorporated into a multilayered structure, it is heated above the temperature noted by the

Figure 4. Annealed aliphatic polyurethane.

endotherms in figure 2. This results in the composite interlayer having properties representative of the thermally annealed state. In order to replicate conditions seen in the final product of laminate structures, samples of polyurethane were heated in an oven at 120 °C for 2 hr to thermally anneal them. In this report, the term annealed refers to having undergone the heat treatment described above whereas the term as drawn refers to the condition straight from the roll.

2.3   Dynamic Mechanical Analysis

Dynamic mechanical analysis (DMA) was performed using a TA Instruments DMA Q800 to determine the storage modulus (E') and the loss modulus (E'') as a function of temperature. DMA allows the user to analyze how the molecular relaxations and modulus of a material are affected by temperature and frequency. Although the small strain measurements from DMA differ from the high-strain processes the material is designed to undergo, various researchers have suggested that DMA can be used to infer yield failure in many thermoplastics (*7*).

Rectangular samples, with approximate dimensions of $34 \times 12 \times 1.27$ mm were cut from the TPU sheets and analyzed in the double cantilever bending mode with a gage length of 8 mm. All samples were scanned from a temperature sweep of -100 to 60 °C at a constant heating rate of 2 °C per min. The resulting plots for E', E'', and tan delta (tan δ) as a function of frequency at 1 Hz are displayed in figures 5–7.

To fully characterize the viscoelastic properties of the material in the frequency domain using linear viscoelastic theory, multiple-frequency sweeps with DMA were performed. From the loss modulus results shown in figure 6, the soft segment glass transition temperatures for each TPU can be taken from the α-relaxation peak maximums. IM 800, IM 1600, IM 2500, and Deerfield 4700 show contributions from secondary β- relaxations, which are not well resolved from the

5
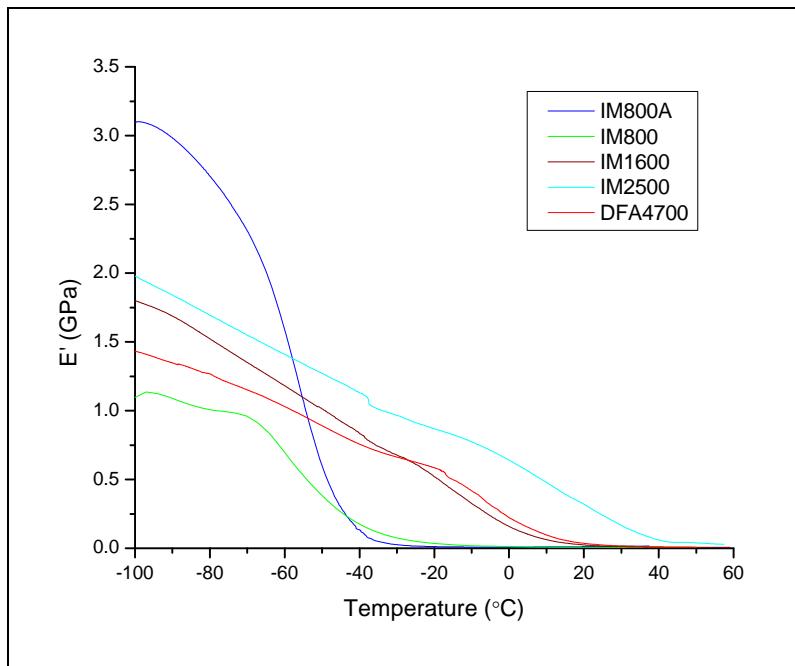
Figure 5. *E*' vs. temperature for the TPU's.
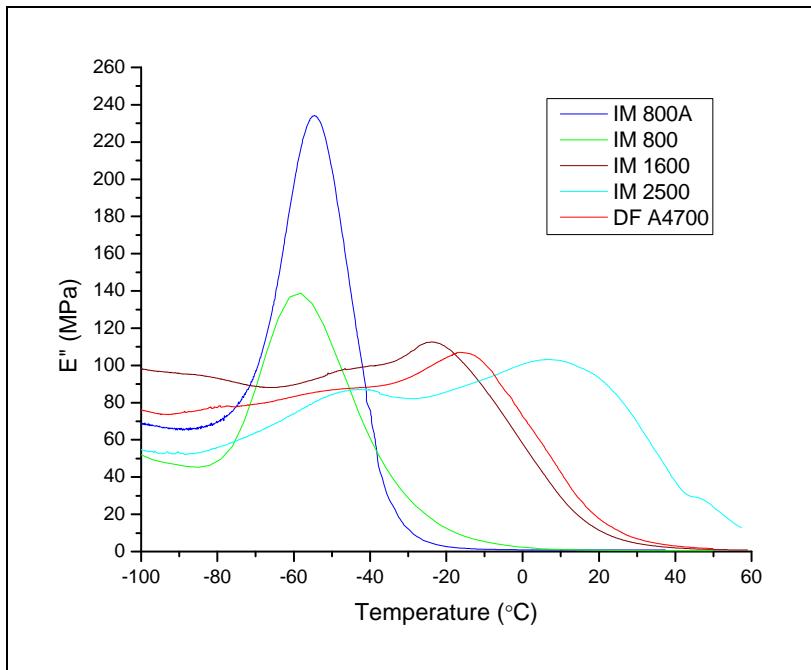

Figure 6. *E*'' vs. temperature for the TPU's.
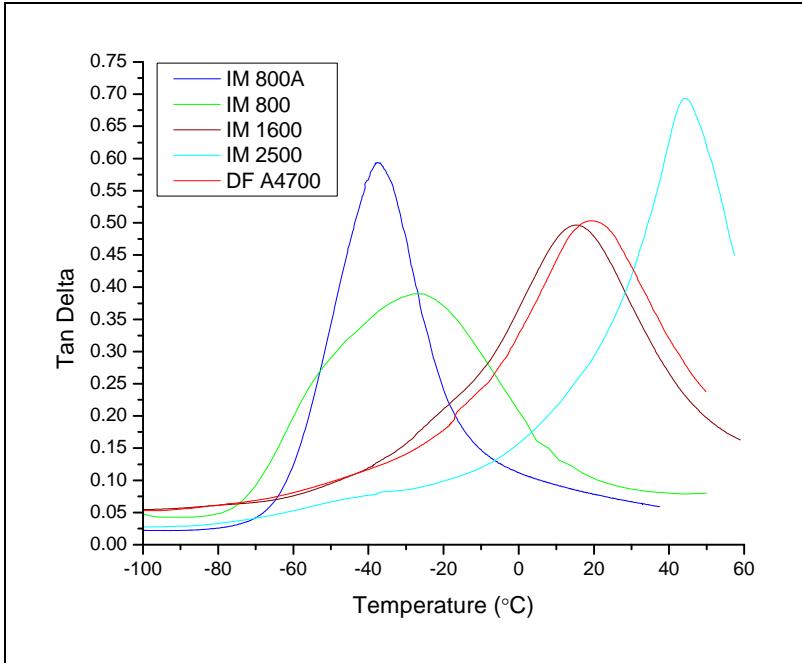
Figure 7. Tan delta for the TPU's.

primary α- relaxation peak. Frequency temperature superposition can be used to resolve secondary glassy β- relaxations from the longer range α- relaxation only if the secondary relaxation peaks are well resolved (*8*). IM 800A is the only TPU where the α- relaxation peak is well resolved from secondary β- relaxation so it was further analyzed with this method.

IM 800A was analyzed with DMA in a multiple-frequency sweep at temperatures from −100 to 50 °C. The sample was equilibrated at a temperature of −100 °C for 5 min, then incremented in steps of 3 °C to a final temperature of 50 °C. At the initiation of each isothermal step the instrument was allowed to equilibrate for 5 min prior to recording a frequency sweep. A frequency sweep of 0.1, 0.3, 1, 3, 10, 30, 50, and 100 Hz was then conducted. At each temperature and frequency, E', E'', and tan δ were recorded. Figures 8 and 9 show E' and E'' spectra, respectively, for the IM 800A TPU obtained from the multiple-frequency sweeps.

From the multi-frequency E' curves, the data from each isotherm can be plotted and horizontally shifted into a single master curve. This single curve represents a much wider frequency range at a single reference temperature. This temperature reduction of the storage modulus is performed by multiplying the storage modulus, E', by (T_0/T), where T_0 is the reference temperature and T is the temperature of the isotherm, and plotting against ωa_T, where ω is the frequency and a_T is the shift factor (*9*). This creates a single curve in which all of the data is reduced to the reference temperature, T_0. Figure 10 shows the unshifted isothermal E' data for the IM 800A TPU. The reference temperature, T_0, for horizontal shifting was set to the glass transition

7
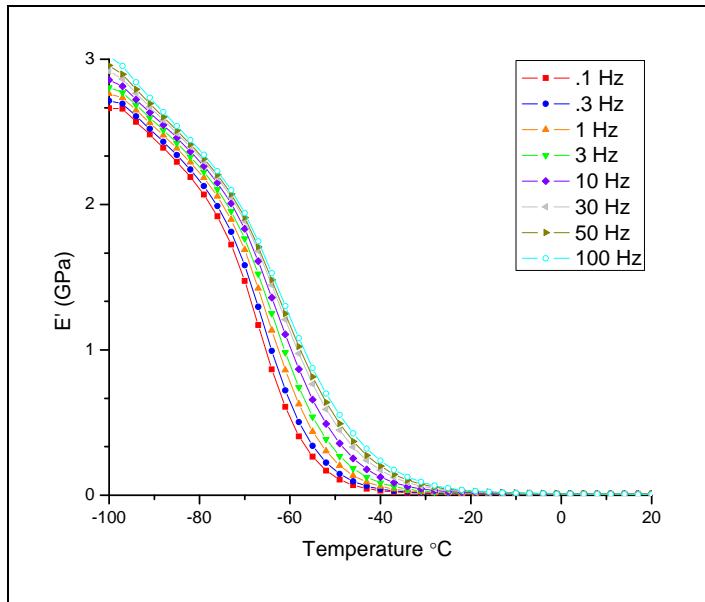
Figure 8. DMA E' curves for IM 800A as a function of
temperature and frequency.
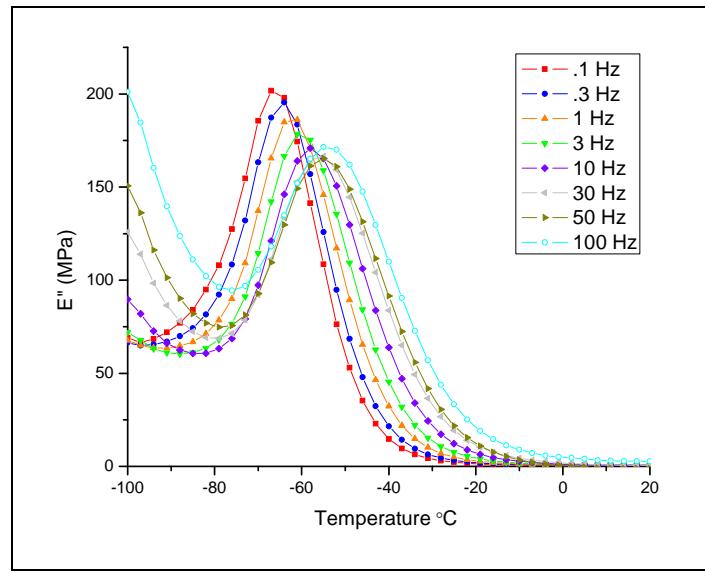
Figure 9. DMA E'' curves for IM 800A as a function of
temperature and frequency.

temperature, $T_0 = T_g = -61\,^{\circ}\text{C}$, determined from the peak of the loss modulus at 1 Hz. By
horizontally shifting the isotherms along the frequency axis and visually aligning each with
OriginPro* software, the individual isothermal data can be assembled into one continuous master
curve, as shown in figure 11.

---

*OriginPro is a registered trademark of OriginLab Corporation, Northampton MA.
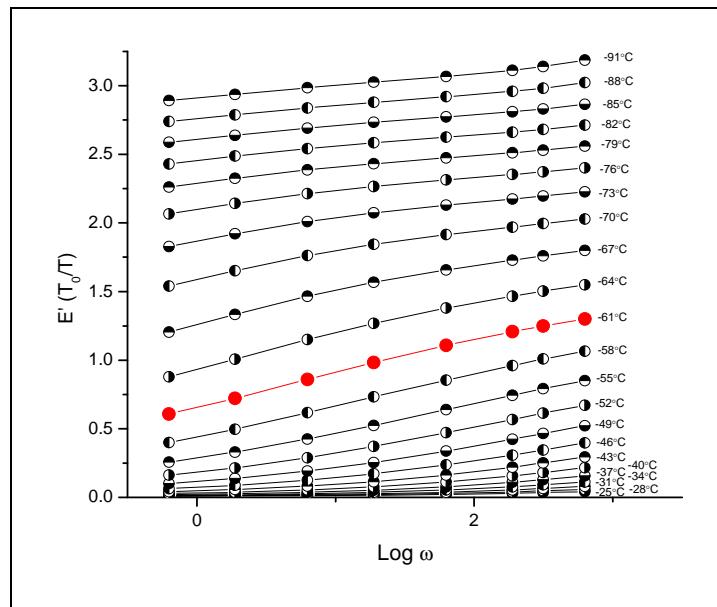
Figure 10. Unshifted *E*' isotherms for IM 800A TPU.
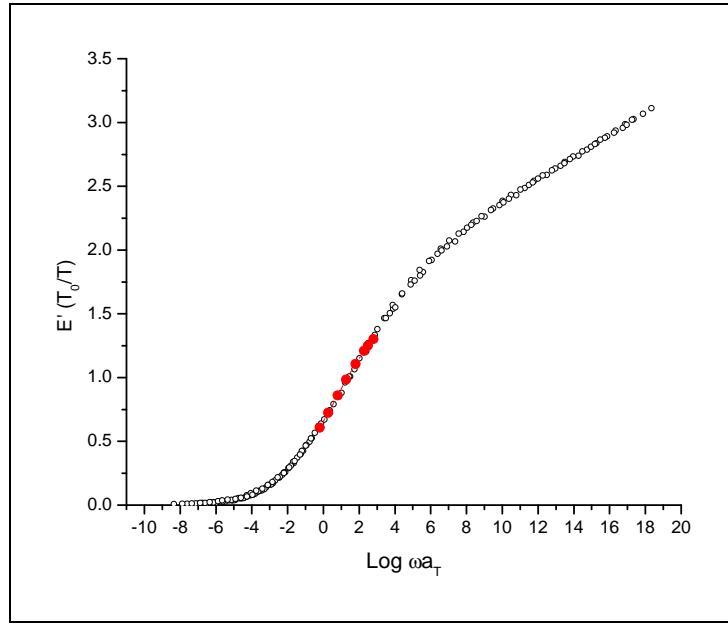
Figure 11. Frequency domain *E*' mastercurve for IM 800A TPU,
             $T_0 = -61°C$ (in red).

The horizontal shift factors (a_T) shift factors from each isotherm can then be used to determine the C_1 and C_2 constants in the WLF equation, where C_1 is dimensionless, and C_2 has units of K.

$$Log\ a_T = \frac{-C_1(T - T_0)}{C_2 + (T - T_0)}.$$ (1)

The WLF constants for the IM 800A TPU were calculated to be $C_1 = 23.1$ and $C_2 = 69.3$ K. As shown in figure 12, the WLF equation with the calculated constants fits the shift factor plot very well. The derived WLF constants are also comparable to the universal constants of 17.4 and 51.6 K.
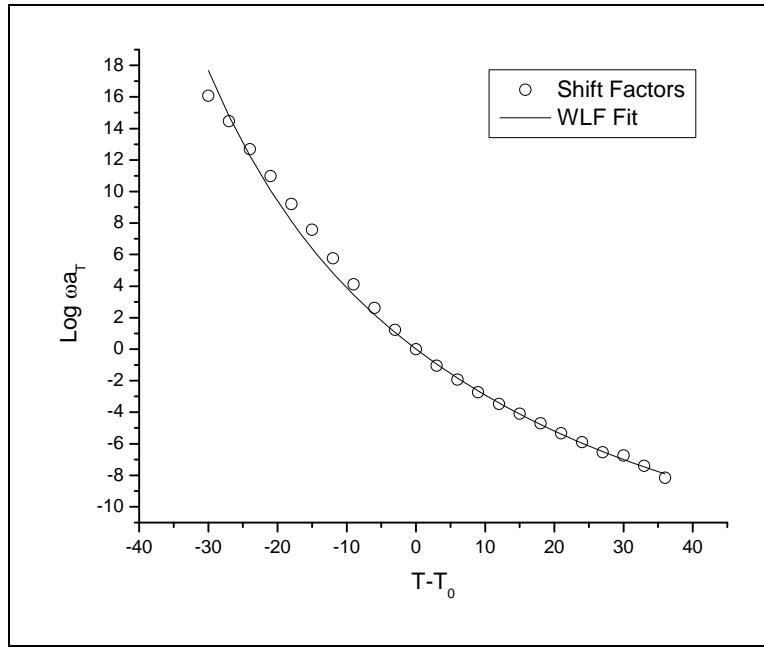
Figure 12. Shift-factor plot and WLF fit of IM 800A E' mastercurve.

Using multi-frequency DMA, the storage modulus master curve was previously generated (figure 11). Master curves produced by DMA are in the frequency domain, and must be converted to the time domain to determine rate-dependent material behavior. The Prony series representation is one method of expressing the numerical interpretation of these master curves that allows simple interconversion between the frequency and time domains. The characteristic equations of the Prony series utilize the same Prony coefficients, E_i, and retardation times, ρ_i, to express the viscoelastic response of a material. E' and E'' can be expressed by the following Prony series representations in the frequency domain (10), where E_e is the equilibrium modulus.

$$E'(\omega) = E_e + \sum_{i=1}^{m} \frac{\omega^2 \rho_i^2 E_i}{\omega^2 \rho_i^2 + 1}.$$ (2)

$$E''(\omega) = \sum_{i=1}^{m} \frac{\omega \rho_i E_i}{\omega^2 \rho_i^2 + 1}.$$ (3)

In the time domain, the Prony series representation of the relaxation modulus is

$$E(t) = E_e + \sum_{i=1}^{m} E_i e^{-\left(t/\rho_i\right)}.$$ (4)

The three Prony series representations shown utilize the same Prony coefficients ($E_1, E_2, E_3, ... E_m$), and retardation times ($\rho_1, \rho_2, \rho_3, ..., \rho_m$), and result in a simple interconversion between time and frequency domains. By extracting the Prony series coefficients from fitting equation 2 to the master curve, shown in figure 11, the complete viscoelastic behavior of the material in both the time and frequency domain can be determined. This extraction was performed by using a linear fit program in Mathematica.[*] The Prony coefficients for the storage modulus determined from DMA of polyurethane are shown in table 1. The equilibrium modulus, E_e, was 0.008517 for this series.

Table 2. Term Prony coefficients for IM 800A from DMA.

i	ρ_i	E_i
1	1.0E-18	0.085322
2	1.0E-17	0.098993
3	1.0E-16	0.079949
4	1.0E-15	0.095701
5	1.0E-14	0.07749
6	1.0E-13	0.091375
7	1.0E-12	0.082454
8	1.0E-11	0.096424
9	1.0E-10	0.094707
10	1.0E-09	0.098849
11	1.0E-08	0.121397
12	1.0E-07	0.107407
13	1.0E-06	0.16329
14	1.0E-05	0.159277
15	1.0E-04	0.200759
16	1.0E-03	0.221608
17	1.0E-02	0.229088
18	1.0E-01	0.246223
19	1.0E+00	0.22039
20	1.0E+01	0.200045
21	1.0E+02	0.14893
22	1.0E+03	0.095498
23	1.0E+04	0.057253
24	1.0E+05	0.02438
25	1.0E+06	0.01394
26	1.0E+07	0.004978
27	1.0E+08	0.002275

[*]Mathematica is a registered trademark of WolframResearch, Inc., Champaign, IL.

Using the Prony coefficients determined from the experimental master curves, the series expansion of equation 2 was performed to generate the elastic modulus as a function of frequency. This function was plotted along with the experimental data it was derived from in figure 13. From looking at this plot, it is clear that the Prony series fits the experimental data extremely well. Next, by using equation 4, the relaxation modulus was determined using the Prony series coeffiecients (figure 14).
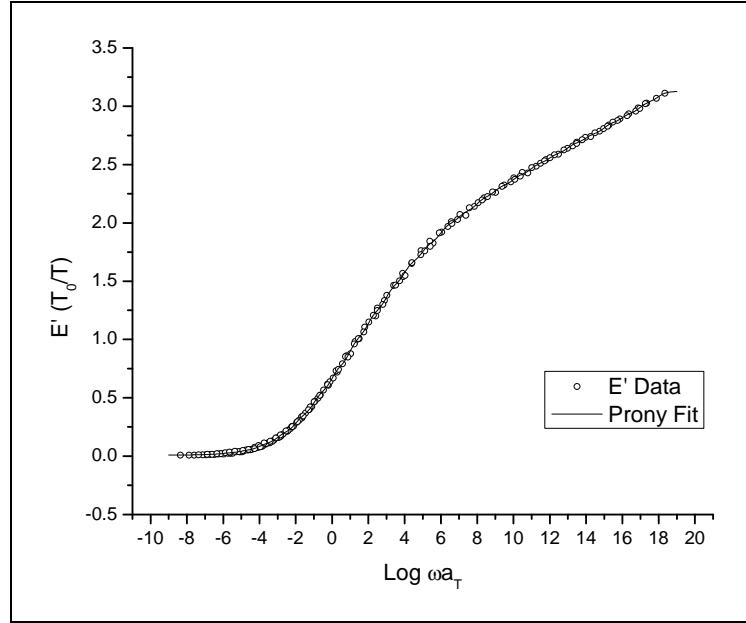

Figure 13. Prony fit of experimental E' frequency domain
mastercurve for IM 800A, $T_0 = -61$ °C.
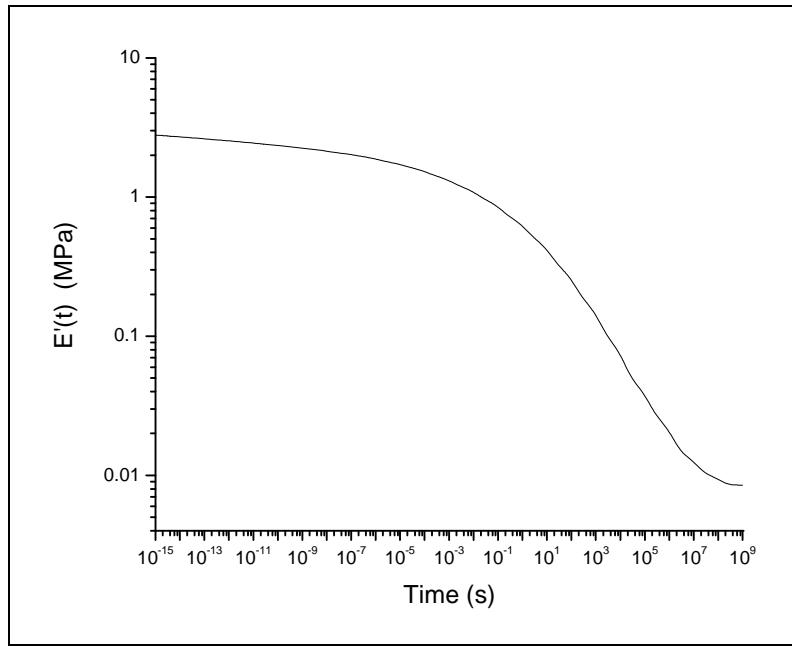
Figure 14. Relaxation modulus from Prony fit of IM 800A, $T_0 = -61$ °C.

2.4   Shear Rheometer

A TA instruments AR 2000 shear rheometer was used to characterize the dynamic shear modulus of the IM 800A TPU. The temperature was incremented in steps of 3 °C from an initial temperature of −85 °C to a final temperature of 50 °C. At each temperature step the sample was held at an isotherm for ~5 min, then a frequency sweep of 1, 3.162, 10, 31.62, and 100 Hz was performed. Figures 15 and 16 show the multi-frequency shear storage modulus (G') and the shear loss modulus (G''), respectively. Next, the temperature reduced isotherms from the multi-frequency shear rheometer tests were horizontally shifted to assemble one continuous master curve, as shown in figure 17.
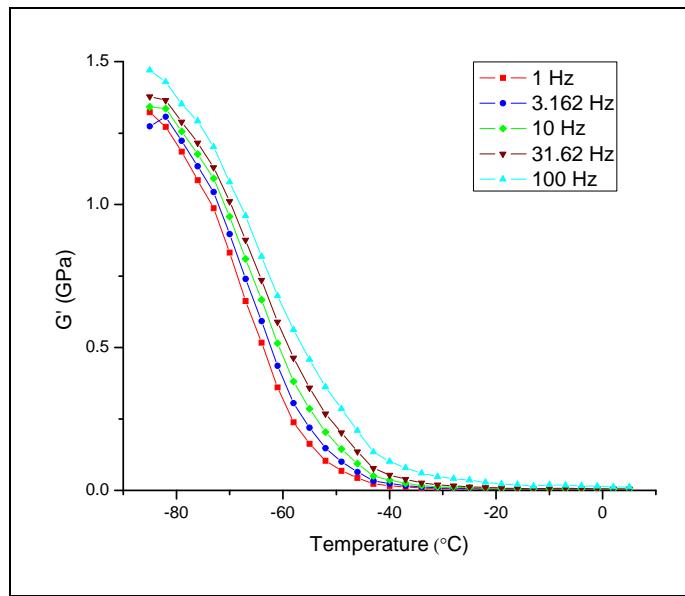

Figure 15. Rheometer G' curves for IM 800A as a function of
temperature and frequency.

Using the WLF equation (equation 1) and a reference temperature of $T_0 = T_g = -61\ {}^\circ\mathrm{C}$, the corresponding WLF constants were found to be $C_1 = 19.8$ and $C_2 = 69.8\ \mathrm{K}$, as shown in figure 18. These values are very close to those calculated from the previous E' data, which is consistent with probing the same underlying molecular relaxation mechanism responsible for the transition.

Next, the Prony series was calculated from the shear storage data by fitting equation 2 to the shifted G' master curve. Table 3 contains the retardation times and Prony coefficients for IM 800A in shear. The equilibrium modulus, G_e, was 0.001124 for this series. Using the Prony coefficients shown in table 3, the Prony fit of the G' curve is plotted with the experimental data in figure 19.
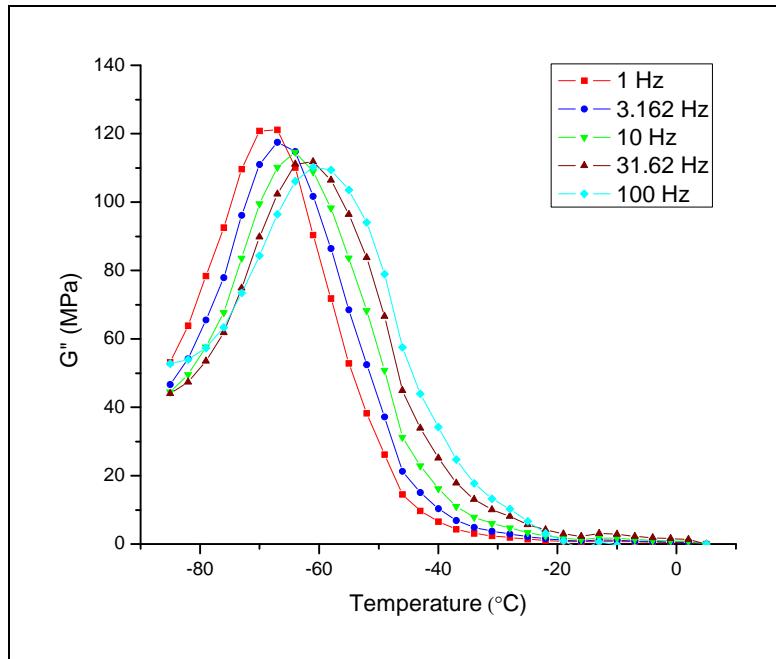
Figure 16. Rheometer G'' curves for IM 800A as a function of temperature and frequency.
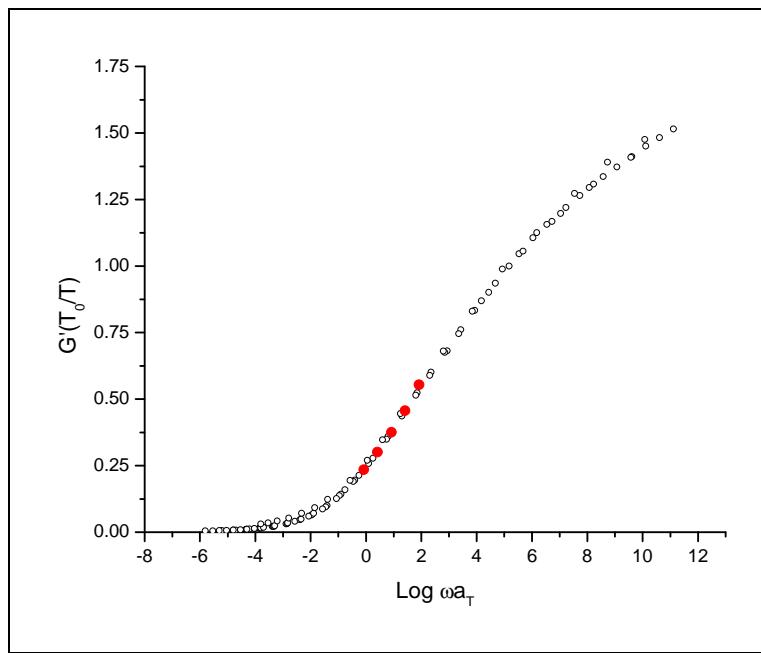
Figure 17. Frequency domain G' mastercurve for IM 800A TPU, $T_0 = -61$ °C.
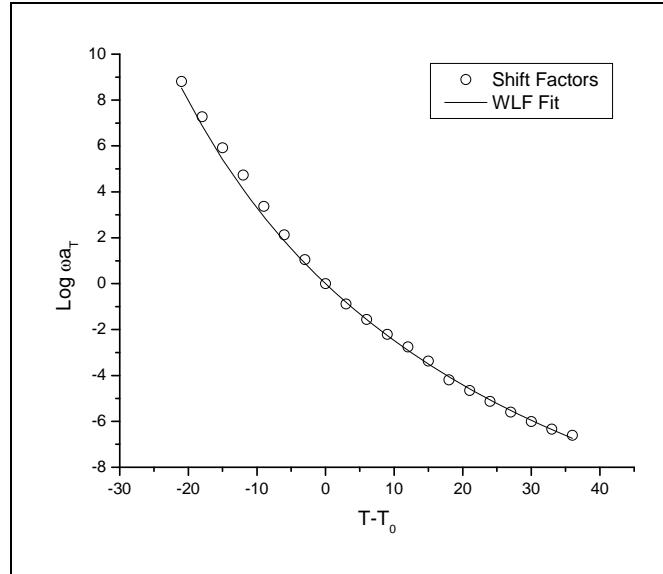
Figure 18. Shift-factor plot and WLF fit of IM 800A *G'* mastercurve, $T_0 = -61$ °C.

Table 3. The 18-term Prony coefficients for IM 800A from shear rheometer.

I	ρ_i	G_i
1	1.0E-11	0.03787
2	1.0E-10	0.083604
3	1.0E-09	0.061284
4	1.0E-08	0.095743
5	1.0E-07	0.097029
6	1.0E-06	0.106472
7	1.0E-05	0.126741
8	1.0E-04	0.148201
9	1.0E-03	0.142998
10	1.0E-02	0.154088
11	1.0E-01	0.157306
12	1.0E+00	0.133704
13	1.0E+01	0.090088
14	1.0E+02	0.047886
15	1.0E+03	0.021599
16	1.0E+04	0.01591
17	1.0E+05	0.002009
18	1.0E+06	0.004623

15
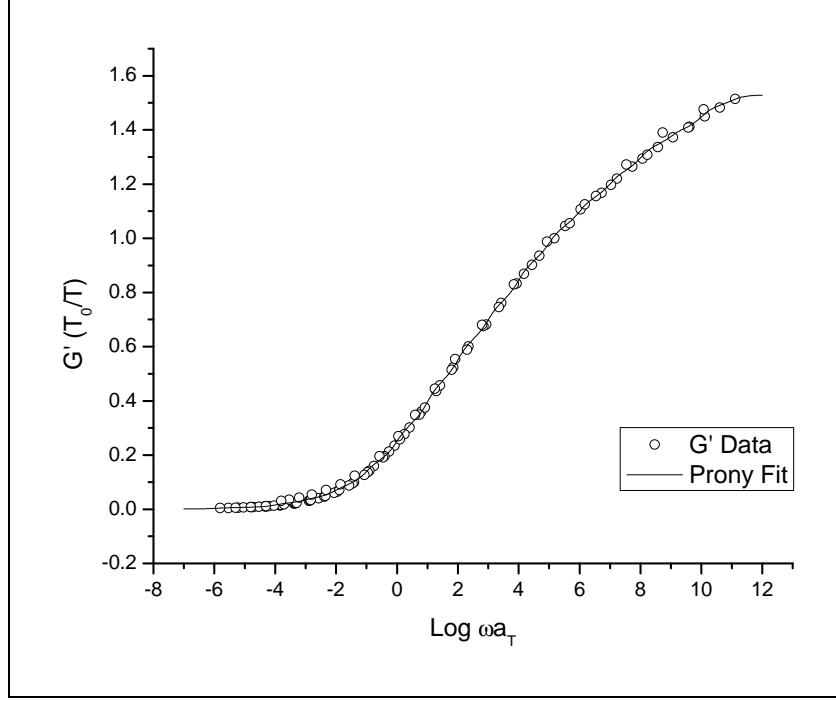
Figure 19. Prony fit of rheometer shear storage modulus data, $T_0 = -61$ °C.

2.5   Activation Energies

From multiple frequency sweeps with DMA and shear rheometry, the activation energies can be determined (*11*). The α-peaks from the loss modulus, representing the segmental motion of the polymer, will shift with temperature as a function of frequency. The extent of the of shift is dependent on the Arrhenius activation energy. The Arrhenius activation energy can be determined from the following equation, where ω is the frequency, E_a is the activation energy, R is the universal gas constant, and T is the absolute peak temperature:

$$\log \omega = \frac{-E_a}{2.303R}\left(\frac{1}{T}\right).$$
(5)

The peaks of the elastic and shear loss moduli and their corresponding temperatures were used in the Arrhenius equation to determine the activation energies. Figure 20 shows the plots for both elastic and shear cases using equation 5.

The activation energy can also be derived from the WLF equation as given by equation 6, where E_a is the activation energy, R is the universal gas constant, a_T is the shift factor, and T is the temperature of the isotherm of the given shift factor.

$$E_a = 2.303R\left(\frac{d\left(\log a_T\right)}{d\left(\frac{1}{T}\right)}\right)_{T=T_0}.$$
(6)

16
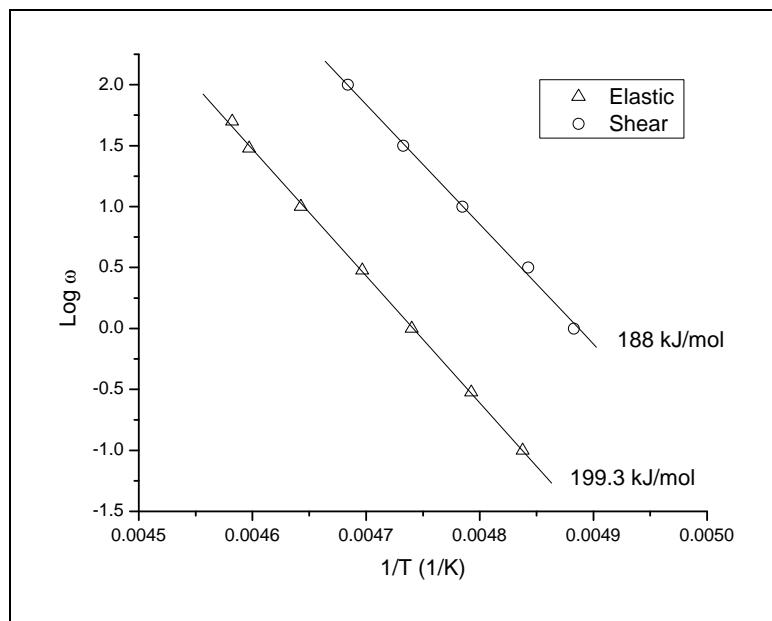
Figure 20. Arrhenius activation energies of IM 800A.

The reference temperature is set to the glass transition temperature of $T_0 = -61$ °C. The activation energies using this alternative form with the calculated shift factors for both elastic and shear cases, are shown in figure 21. The activation energies calculated using this alternative method are very close to those previously determined from the Arrhenius method.
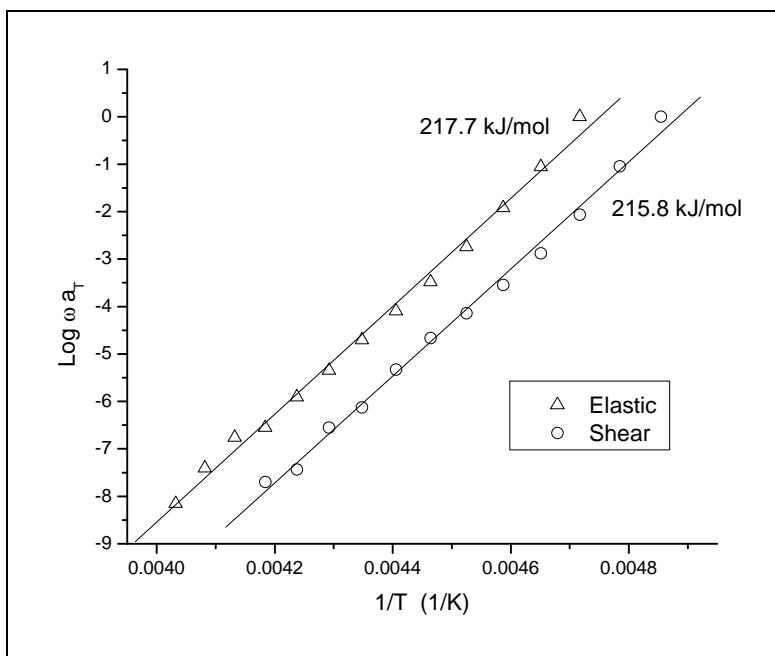
Figure 21. Alternative expression for activation energies of IM 800A.

17

2.6   Mechanical Testing

To determine the mechanical properties of IM 800A, tensile and compression tests were performed. The tensile strength was tested as a function of both the orientation direction and heat treatment. Dog-bone samples of TPU were cut from both as drawn and thermally annealed sheets of 1.27-mm-thick IM 800A. The samples were cut both parallel and perpendicular to the draw direction using a Hudson Hydraulic Mini-Clicker model no. S108.

Tensile tests of dog-bone samples were performed using an Instron 4505 equipped with a 1-kN load cell. Tensile samples were strained until failure. The strain of the specimen was determined from the crosshead displacement. The crosshead speed was 228.6 mm/min with a gage length of 38.1 mm, resulting in a strain rate of ~0.1 s^{-1} (figure 22).

From the tensile tests, there is a clear distinction between the as drawn and thermally annealed samples, as noted with the dashed and solid lines in figure 22. This suggests that thermally annealing the polymer significantly affects the mechanical properties. Within each heat treatment, samples were tested parallel and perpendicular to the draw direction. The sample average ultimate tensile strength (UTS), stress at 100% strain, and strain-to-failure percentage are highlighted in table 4. From these figures, there is a clear distinction between annealed and as-drawn samples. However, the draw orientation showed no significant effects on the tensile properties of IM 800S, leaving it safe to assume the material is isotropic.
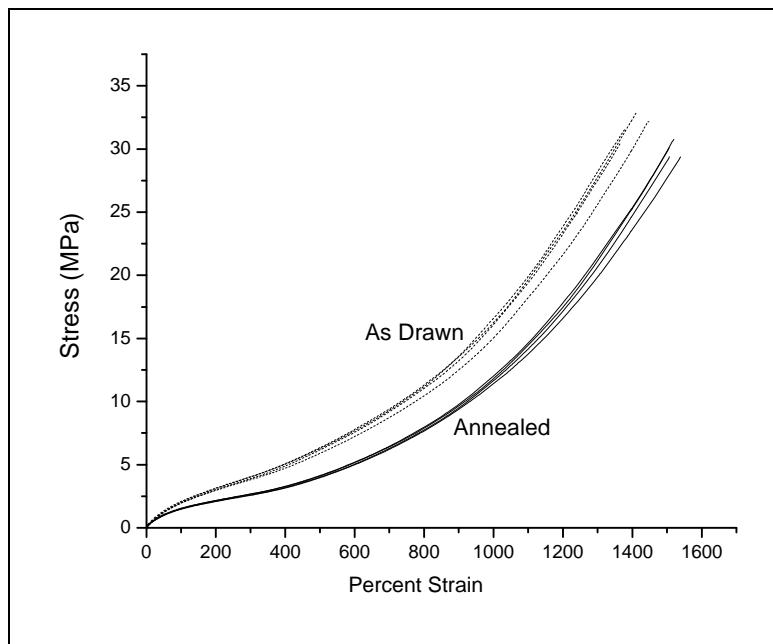

Figure 22. Tensile tests of IM 800A.

Table 4. Mechanical characteristics from tensile tests of IM 800A.

Treatment	Orientation	UTS (MPa)	Strain-to-Failure (%)	Stress at 100% Strain (MPa)
As drawn	Perpendicular	31.4	1406	1.95
As drawn	Parallel	32.3	1395	2.06
Annealed	Perpendicular	29.4	1523	1.49
Annealed	Parallel	30.4	1513	1.54

To perform compression tests on IM 800A, 25.4-mm-diameter circular samples were cut from as-drawn and annealed IM 800A. The circular cut-outs, having a thickness of ~1.27 mm, were then stacked in groups of 10 creating a total thickness of 12.7 mm. Since the tension tests showed that the mechanical strength of the material is not significantly affected by the orientation of the sample, the draw direction was disregarded in the compression tests. Silicone grease was used to lubricate contact surfaces of the sample to reduce friction and prevent barreling. Compression tests were performed using an Instron 4505 with 5-kN load cell. Specimens were compressed until the engineering strain was 5. The crosshead speed was 1.27 mm/min which resulted in a strain rate of ~0.002 s^{-1}. The resultant plot of engineering stress as a function of percent strain is shown in figure 23.
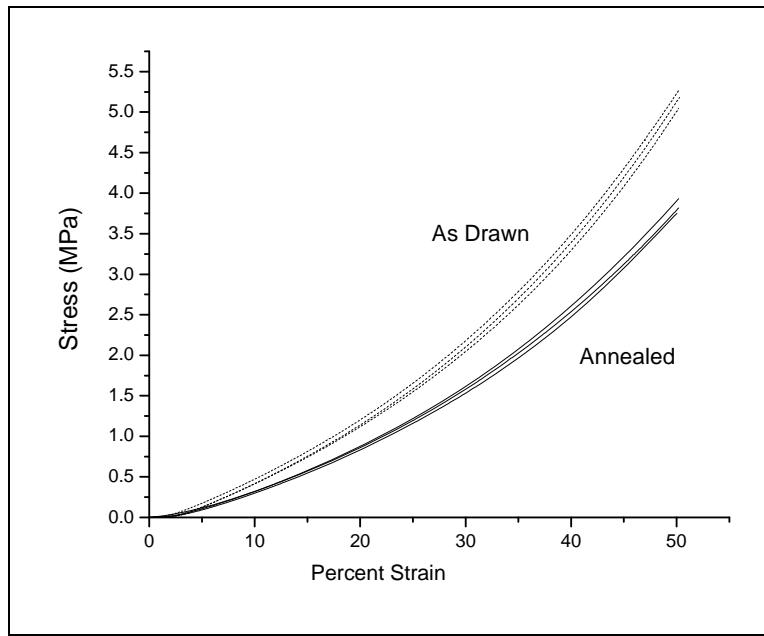

Figure 23. Compression tests of cylindrical IM 800A. T = 25 °C.

Visual image correlation (VIC) was used during mechanical testing to quantify the three dimensional strains in the specimen. VIC-Snap and VIC-3D software from Correlated Solutions was used for image processing and strain computations. VIC utilized two cameras mounted at

differing angles to measure the three-dimensional (3-D) movements of a painted pattern on the sample as it is deformed. VIC simultaneously captures both perpendicular and parallel strain to the direction of the applied load with a very high resolution, which is useful for deriving Poisson's ratios. The VIC methodology also eliminates the experimental difficulty of attaching strain gages to the test specimens. One drawback of using VIC is that it is limited by the amount of deformation present in the sample, which occurs when the painted pattern begins to crack.

The tensile test strain data from VIC did not have enough points to accurately determine the strains in the linear region of the test due to the painted pattern cracking. However, VIC from compression tests resulted in a more accurate representation of the 3-D strain state. By plotting the X and Y strains in a plane tangent to the cylinder's surface, the Poisson's ratio of the material can be easily determined (figure 24). For the compression tests, the Poisson's ratio for both as drawn and annealed samples was ~0.49. This value is a typical value for elastomers and reflects a near incompressibility for these quasi-static tests.
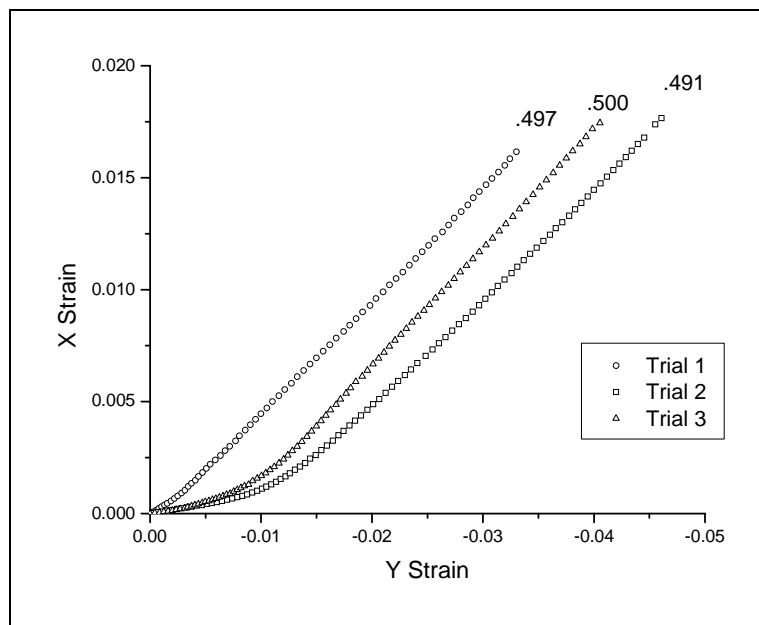

Figure 24. Perpendicular (X) strain vs. parallel (Y) strain during compression for IM 800A TPU as determined by VIC analysis. T = 25 °C.

An Instron SFL 3119 series temperature-controlled chamber was used to conduct a chilled compression testing using an Instron 1125 testing frame equipped with a 22.2-kN load cell. A schematic of the equipment used for the cooled compression test is shown in figure 25. Liquid nitrogen was used to cool compression samples to –75 °C. Since the glass transition temperature of IM 800A is –61 °C, it was necessary to chill the sample below this temperature to significantly change the elastic modulus. Each sample was equilibrated at –75 °C with

compression plates touching both faces of the specimen for 5 min to minimize the effects of thermal gradiants. During the cooled compression tests, the test was stopped when the load in the sample reached 20 kN.
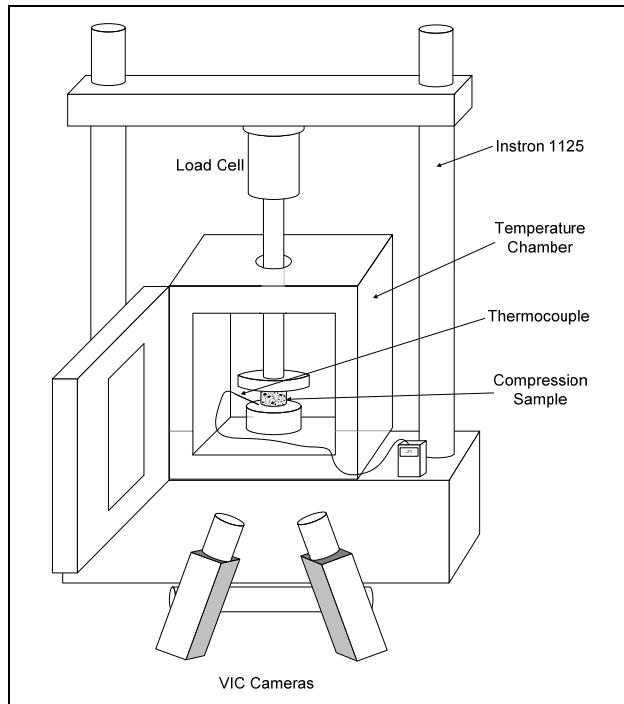

Figure 25. Equipment setup for cooled compression test.

Figure 26 shows the engineering stress as a function of strain for the cooled compression tests. By comparing these compression tests with those done at room temperature, the extent to which temperature affects the modulus of the material can be seen. There is a significant amount of scatter in the data that may have been caused by a number of factors: Dynamic mechanical analysis revealed that at this temperature, a temperature difference of only 3 °C will change the modulus of IM 800A by ~170 MPa. Figure 27 shows the experimental ranges of stress at 20% strain for each of the mechanical tests performed.

The experimental perpendicular and parallel strain data obtained from VIC at sub-ambient temperature was not as sharply defined as the room temperature compression test results. However, a linear fit of the initial region resulted in a Poisson's ratio of ~0.36 for both as drawn and annealed samples (figure 28), which is a value well within reason for glassy polymers.
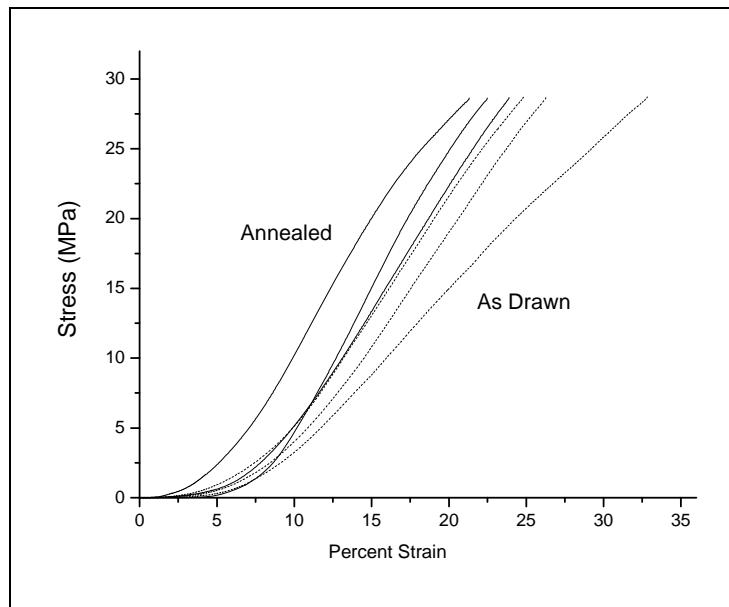
Figure 26. Cooled compression tests of cylindrical IM 800A.
   T = –75 °C.
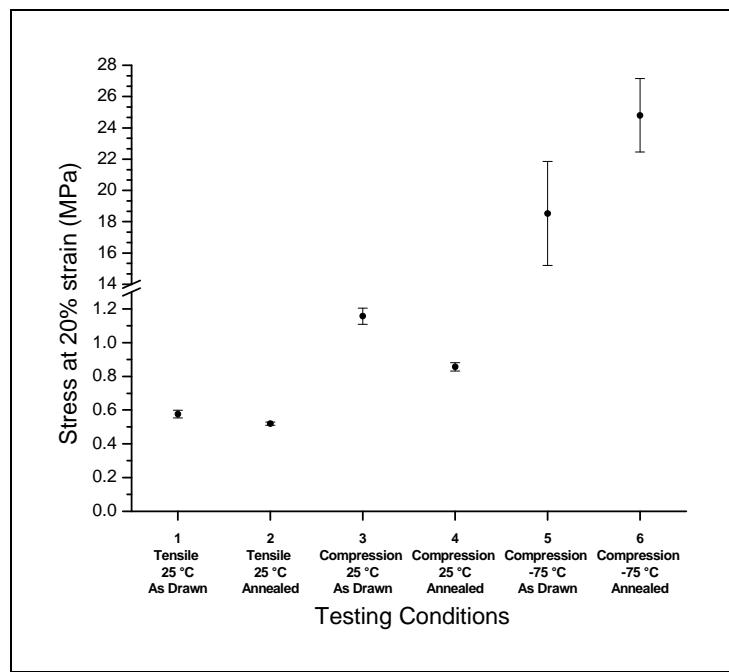

Figure 27. Stress at 20% strain for mechanical testing.
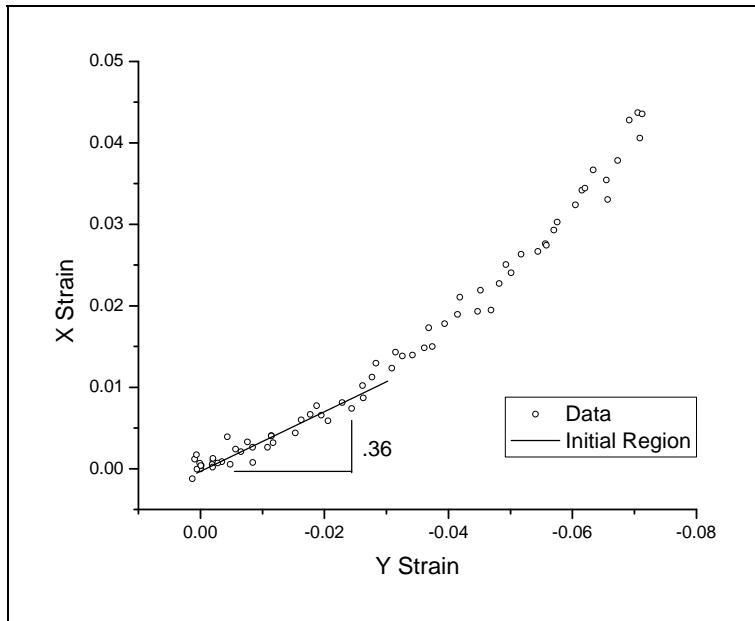
Figure 28. Perpendicular (X) strain vs. parallel (Y) strain during
compression for IM 800A TPU as determined by VIC
analysis. T = –75 °C.

3.   Conclusion

To characterize the properties of interlayer materials commonly used in transparent laminated structures, five different commercially available aliphatic TPU's were studied. By using DMA to analyze the TPU's, Inter Materials IM 800A was determined to be the only TPU to have a well resolved α-peak in the loss modulus, lending to traditional linear viscoelasticity characterization. Utilizing multi-frequency sweeps with DMA and shear rheometry, the WLF constants and Prony series coefficients for elastic and shear cases were determined for annealed IM 800A.

Mechanical tests were performed to determine the tensile and compressive properties at room temperature and in a cooled environment. The Poisson's ratio determined by VIC of 0.49 correlates well to the Poisson's ratio of typical rubbers. Cooled compression tests revealed a lower Poisson's ratio of 0.36, and a much higher elastic modulus.

Additional studies on this material that could be potentially beneficial in determining its usefulness as an interlayer would be testing adhesive strength and its influence on stress wave propagation through dissimilar materials during high rate loading. Further mechanical testing incorporating unloading curves to determine the extent of plastic strain would also be very

useful. Also, instrumenting a sample with biaxial extensometers in a tensile test would allow the calculation of Poisson's ratio of the material at high deformations where VIC was determined to be limited. Furthermore, the characterizing of other TPU's would allow the comparison of the performance of different materials when their properties are known.

4. References

1. Martinez, M. A.; Rodriguez, J.; Sanchez Galvez, V.; Sastre, L. A. Confined Compression of Elastic Adhesives at High Rates of Strain. *International Journal of Adhesion and Adhesives* **1998**, *18* (6), 375–383.

2. Abrate, S. *Impact on Composite Structures*. Press Syndicate of the University of Cambridge: Cambridge, UK, 1998, 289.

3. Bowden, F. P. The Brittle Fracture of Solids by Liquid Impact, by Solid Impact, and by Shock. *Proc. R Soc. London A* **1964**, 282, 331–352.

4. Tasdemirci, A. Experimental and Modeling Studies of Stress Wave Propagation in Multilayer Composite Materials: Low Modulus Interlayer Effects. *Journal of Composite Materials* **2005**, *39*, (11), 981–1005.

5. Martin, D. J.; Guntillake, P. A.; Yozghatlian, S. P.; Renwick, G. M. The Influence of Composition Ratio on the Morphology of Biomedical Polyurethanes. *Journal of Applied Polymer Science* **1997**, *71* (6), 937–952.

6. White, J. R. Polymer Ageing: Physics, Chemistry, or Engineering? Time to Reflect. *C. R. Chimie* **2006**, *9* (11–12), 1396–1408.

7. Bauwens, J. C. Relation Between the Compressive Yield Stress and the Mechanical Loss Peak of Bisphenol-A-Polycarbonate in the β Transition Rance. *Journal of Materials Science* **1972**, *7* (5), 577–584.

8. Aklonis, J. J.; Shen, M. *Introduction to Polymer Viscoelasticity*. Wiley-Interscience: New York, NY, 1972.

9. Ferry, J. D. *Viscoelastic Properties of Polymers*; 2nd ed.; John Wiley & Sons: New York, NY, 1970.

10. Park, S.W. Methods of Interconversion Between Linear Viscoelastic Material Functions. Part 1 - A Numerical Method Based on Prony Series. *International Journal of Solids and Structures* **1997**, *36* (41), 1653–1675.

11. Jensen, R. E.; McKnight, S. H. Viscoelastic Properties of Alkoxy Silane-Epoxy Interpenetrating Networks. *International Journal of Adhesion and Adhesives* **2005**, *26* (1–2), 103–115.

NO. OF
COPIES ORGANIZATION

  1   DEFENSE TECHNICAL
 (PDF   INFORMATION CTR
 ONLY)   DTIC OCA
         8725 JOHN J KINGMAN RD
         STE 0944
         FORT BELVOIR VA 22060-6218

  1   US ARMY RSRCH DEV &
         ENGRG CMD
         SYSTEMS OF SYSTEMS
         INTEGRATION
         AMSRD SS T
         6000 6TH ST STE 100
         FORT BELVOIR VA 22060-5608

  1   DIRECTOR
         US ARMY RESEARCH LAB
         IMNE ALC IMS
         2800 POWDER MILL RD
         ADELPHI MD 20783-1197

  3   DIRECTOR
         US ARMY RESEARCH LAB
         AMSRD ARL CI OK TL
         2800 POWDER MILL RD
         ADELPHI MD 20783-1197

         ABERDEEN PROVING GROUND

  1   DIR USARL
         AMSRD ARL CI OK TP (BLDG 4600)

ABERDEEN PROVING GROUND

    6   DIR USARL
         AMSRD ARL WM MA
           M VANLANDINGHAM
           R JENSEN
           A BUJANDA
         AMSRD ARL WM MD
           J SANDS
           P PATEL
         AMSRD ARL WM TD
           T WEERASOORIYA

INTENTIONALLY LEFT BLANK.